

BBAMEM 75863

## Effects of platelet-activating factor and related lipids on dielaidoylphosphatidylethanolamine by DSC, FTIR and NMR

Josefa Salgado, José Villalaín and Juan C. Gómez-Fernández

*Departamento de Bioquímica y Biología Molecular A, Facultad de Veterinaria, Universidad de Murcia, Murcia (Spain)*

(Received 1 June 1992)

(Revised manuscript received 8 October 1992)

**Key words:** 1-Palmitoylphosphatidylcholine; Lyso-PAF; PAF; Hexagonal H<sub>II</sub> phase; DSC; NMR, <sup>31</sup>P-

The effect of platelet-activating factor (1-*O*-hexadecyl-2-acetyl-*sn*-glycero-3-phosphocholine, PAF) and two related molecules, 1-*O*-hexadecyl-*sn*-glycero-3-phosphocholine (LPAF) and 1-palmitoyl-*sn*-glycero-3-phosphocholine (LPC) on dielaidoylphosphatidylethanolamine (DEPE) lipid structure and polymorphism has been studied by differential scanning calorimetry (DSC), Fourier transform infrared (FTIR) and <sup>31</sup>P nuclear magnetic resonance (<sup>31</sup>P-NMR) spectroscopies. From the interaction of these molecules with DEPE it is concluded that all of them stabilize the lamellar phase with respect to the hexagonal H<sub>II</sub> phase and this effect is clear even at concentrations of these compounds as low as 1 mol%. It is also shown that, although they perturb the gel to liquid-crystalline phase transition of DEPE up to a similar extent, fluidizing the membrane, PAF but not LPAF or LPC, induces the presence of more than one peak in the calorimetric profile. Moreover, FTIR data indicate that lateral phase separations formed by PAF-rich phases are taking place. Remarkably,  $\Delta H$  of the main transition decreases at concentrations lower than 2 mol% but remains nearly constant up to 30 mol%. <sup>31</sup>P-NMR measurements showed that all these molecules were capable of inducing isotropic signals in the spectra produced by molecules associated to membranes before micellization of the vesicles.

### Introduction

Platelet-activating factor (PAF) is a naturally occurring alkyl-ether phospholipid with diverse and potent physiological functions. It is an unusual phospholipid differing markedly from the common phosphoglycerides isolated from plasma membranes because of both the ether linkage in the 1-position and the acetyl group in the 2-position of the glycerol backbone. Each

feature of the unusual structure of PAF is important for its optimal biological activity [1].

PAF was first described as a fluid phase mediator of the interaction between leukocytes and platelets [2], activating at nM concentrations systems and functions such as platelets [3], adhesion and degranulation of neutrophils [4], pathways involved in coagulation and inflammation [5], etc. At micromolar or greater concentrations, PAF can induce the differentiation of cultured neurons, macrophage activation and even neuronal death [6–8].

PAF is known to trigger cell activation by a membrane protein receptor [1], but a large non-specific binding of PAF to membranes has impeded for a long time the disclosure of the membrane receptor. It is then highly probable that PAF, a molecule with a high hydrophobicity, interacts with membrane lipids at a certain step of the activation process. PAF is also a member of the asymmetric phospholipid family and this type of lipids are known to form interdigitated phases [9]. Apart from that, PAF has also an ether-linked acyl chain, and lipids bearing such a feature are known to affect the gel to liquid-crystalline phase transition temperature of glycerophosphatides [10,11]. Moreover, PAF and 1-acyl-*sn*-glycero-3-phosphocho-

Correspondence to: J.C. Gómez-Fernández, Departamento de Bioquímica y Biología Molecular A, Facultad de Veterinaria Universidad de Murcia, Apdo. Postal 4021, E-30080 Murcia, Spain.

Abbreviations: DEPE, 1,2-dielaidoyl-*sn*-glycero-3-phosphoethanolamine; dPAF, 1-*O*-[7,7,8,8-<sup>2</sup>H<sub>4</sub>]hexadecyl-2-acetyl-*sn*-glycero-3-phosphocholine; DPPC, 1,2-dipalmitoyl-*sn*-glycero-3-phosphocholine; DSC, differential scanning calorimetry;  $\Delta H$ , enthalpy change of the gel to liquid-crystalline phase transition; FTIR, Fourier transform infrared spectroscopy; LPAF, 1-*O*-hexadecyl-*sn*-glycero-3-phosphocholine (lyso-PAF); LPC, 1-palmitoyl-*sn*-glycero-3-phosphocholine; lyso-PC, 1-acyl-*sn*-glycero-3-phosphocholine; PAF, 1-*O*-hexadecyl-2-acetyl-*sn*-glycero-3-phosphocholine; <sup>31</sup>P-NMR, <sup>31</sup>P nuclear magnetic resonance spectroscopy;  $\Delta\sigma$ , chemical shift anisotropy;  $T_C$ , onset temperature of the gel to liquid-crystalline phase transition;  $T_H$ , onset temperature of the bilayer to hexagonal H<sub>II</sub> phase transition.

lines (lyso-PC) share structural features which give them detergent capacity and hence they may be considered membrane destabilizers. This has been widely shown for lyso-PC [12,13] and also recently for both lyso-PC and PAF [14]. But lyso-PC is also important as a bioactive lipid, which may act as an endothelium relaxant [15] or as a chemotactic factor for human monocytes [16].

In the present study we compare the effects of PAF and two related lipids, 1-*O*-hexadecyl-*sn*-glycero-3-phosphocholine (LPAF) and 1-palmitoyl-*sn*-glycero-3-phosphocholine (LPC), on the physical and polymorphic properties of membranes formed by 1,2-di-elaidoyl-*sn*-glycero-3-phosphoethanolamine (DEPE). Phosphatidylethanolamines represent the second largest phospholipid component in animal membrane lipids after the phosphatidylcholines. They are characterized by their facility to adopt inverted hexagonal  $H_{II}$  phases and it has been shown that the formation of hexagonal phases has a marked effect on biological phenomena [17–19]. The analogs of PAF were chosen in order to evaluate the importance of the 2-position acetyl group and the 1-position ether linkage. The effects of PAF, LPAF and LPC on the physical properties of DEPE have been studied by using three non-perturbing techniques such as  $^{31}\text{P}$  nuclear magnetic resonance ( $^{31}\text{P}$ -NMR), Fourier transform infrared spectroscopy (FTIR) and differential scanning calorimetry (DSC).

## Materials and Methods

### Materials

1-*O*-Hexadecyl-2-acetyl-*sn*-glycero-3-phosphocholine (platelet activating factor, PAF) was obtained from Bachem (Saffron Walden, UK) whereas 1-*O*-hexadecyl-*sn*-glycero-3-phosphocholine (LPAF), 1-palmitoyl-*sn*-glycero-3-phosphocholine (LPC) and 1,2-di-elaidoyl-*sn*-glycero-3-phosphoethanolamine (DEPE) were obtained from Avanti Polar Lipids (Birmingham, AL, USA) and judged chromatographically pure by high performance thin-layer chromatography. 1-*O*-[7,7,8,8- $^2\text{H}_4$ ]hexadecyl-2-acetyl-*sn*-glycero-3-phosphocholine (dPAF) was obtained from Cascade Biochem (Reading, UK). All the other compounds were of analytical grade. Water was twice distilled in an all glass distiller and deionized in a Milli-Q apparatus from Millipore.

### Differential scanning calorimetry

Samples of 3  $\mu\text{M}$  of DEPE and the appropriate amount of PAF, LPAF or LPC in chloroform were dried under a stream of  $\text{O}_2$ -free  $\text{N}_2$ , and the last traces of solvent were removed by high vacuum for more than 3 h. The samples were kept and dispersed for 30 min at 50°C, temperature above the gel to liquid-crystalline phase transition of the mixture, in 500  $\mu\text{l}$  of 0.1 mM

EDTA, 10 mM Mops, 100 mM NaCl buffer (pH 7.4), with occasional mixing in a vortex mixer obtaining a homogeneous and uniform suspension. Subsequently the samples were spun and pelleted at high speed in a bench microfuge. Then the pellets were carefully transferred to small aluminum pans and scanned in a Perkin-Elmer DSC-4 calorimeter using a reference pan containing buffer. The instrument was calibrated using indium as standard. The samples were scanned with a heating and cooling rate of 4  $^\circ\text{C}/\text{min}$  at 1 mcal/s in all experiments. The range of temperatures studied was from 20°C to 80°C. Each sample was scanned five consecutive times and no differences were observed among the results obtained for these scans. Peak areas were measured by weighing paper cut-outs of the peaks. Data was obtained from the thermograms as previously described by Elias et al. [20].

After the measurements, the pans were carefully opened and the samples were dissolved in chloroform/methanol (1:1, v/v). After subsequent perchloric acid hydrolysis, the amount of phospholipid originally present was determined as described before [21].

The incorporation of PAF into liposomes was measured by combining gas-chromatography and phosphorus assay, i.e., aliquots were assayed for phosphorus, and fatty acids were quantitatively assayed using internal standards.

### $^{31}\text{P}$ nuclear magnetic resonance

45  $\mu\text{mol}$  of DEPE and the appropriate amount of PAF, LPAF or LPC were mixed in a final volume of 300  $\mu\text{l}$  of chloroform in a small tube (5 cm length, 8 mm outer diameter) and evaporated to dryness under a stream of  $\text{N}_2$ , followed by 3 h storage under high vacuum to remove last traces of solvent. 200  $\mu\text{l}$  of buffer (0.1 mM EDTA, 10 mM Mops, 100 mM NaCl buffer (pH 7.4)) were added to the obtained lipid film. The samples were kept for 60 min at 50°C to hydrate the phospholipid. The tube was then put inside a conventional 10 mm NMR tube with external  $\text{D}_2\text{O}$ .  $^{31}\text{P}$ -NMR spectra were recorded in the Fourier transform mode on a Bruker AC-200 spectrometer (81 MHz) equipped with an Aspect 3000 computer. Temperature was controlled to  $\pm 1$   $^\circ\text{C}$  with a standard Bruker B-VT-1000 variable temperature control unit. All chemical shift values are quoted in parts per million (ppm) from pure LPC micelles (0 ppm), positive values referring to low-field shifts. All spectra were obtained in the presence of a gated-broad band decoupling (4 W input power during acquisition time) and accumulated free induction decays were obtained from up to 2000–2500 transients. A spectral width of 25 kHz, a memory of 8K data points, a 1.3 s interpulse time and a 80° radio frequency pulse, were used. Prior to Fourier transformation an exponential multiplication was applied resulting in a 100 Hz line broadening.

The residual chemical shift anisotropy,  $\Delta\sigma$ , was measured as 3-times the chemical shift difference between the high-field peak and the position of isotropically moving lipid molecules at 0 ppm [22]. In order to check the formation of small vesicles or micelles from non-incorporated lipids which could give rise to an isotropic resonance in the spectra, samples for  $^{31}\text{P}$ -NMR were prepared and analyzed as described above. After the measurements, the samples were taken and centrifuged at  $5000 \times g$  for 10 min and both the supernatant and pellet were studied separately by  $^{31}\text{P}$ -NMR. Aliquots were also measured by DSC as described above. In all cases the alterations in the NMR spectra were reversible upon recooling the samples.

#### Fourier transform infrared spectroscopy

Samples for Fourier transform infrared spectroscopy containing 3.7  $\mu\text{mol}$  DEPE and the appropriate amount of dPAF in chloroform were dried under a stream of  $\text{O}_2$ -free  $\text{N}_2$  and the last traces of solvent eliminated by desiccation under vacuum for more than 3 h. After the addition of 50  $\mu\text{l}$  of 0.1 mM EDTA, 10 mM Mops, 100 mM NaCl  $\text{H}_2\text{O}$  buffer (pH 7.4), multilamellar liposomes were formed by careful mixing using a bench vibrator and keeping the samples at  $50^\circ\text{C}$ . Mixing was continued until a homogeneous and uniform suspension was obtained. Then, the samples were kept for 30 min at  $50^\circ\text{C}$  with occasional mixing on a vortex mixer.

Infrared spectra were obtained in a Philips PU9800 Fourier transform infrared spectrometer equipped with

a DTGS detector. Samples were examined in a thermostated Specac 20710 cell equipped with  $\text{CaF}_2$  windows and using 25  $\mu\text{m}$  teflon spacers (all from Specac, Kent, UK). Each spectrum was obtained by collecting 250 interferograms with a nominal resolution of  $2\text{ cm}^{-1}$  and triangular apodization using the sample shuttle accessory in order to average background spectra between consecutive sample spectra over the same time period. The spectrometer was continuously purged with dry air in order to remove atmospheric water vapor from the bands of interest. The samples were equilibrated at  $-10^\circ\text{C}$  for 20 min before acquisition. Samples were scanned between  $-10^\circ\text{C}$  and  $58^\circ\text{C}$  at  $2^\circ\text{C}$  intervals with 5 min delay between each consecutive scan with a water bath interfaced to the spectrometer computer. Subtraction from buffer taken at the same temperatures as the sample was performed interactively using Spectra-Calc (Galactic Industries, Salem, USA). Frequencies at the center of gravity were measured by taking the top ten points of each specific band and fitting them to a Gaussian function. Due to the low signal-to-noise ratio of the dPAF bands a 9-point Savitsky-Golay smoothing function was used.

#### Results

The effect of incorporating different amounts of PAF and LPAF, on the thermotropic phase transitions of DEPE as seen by DSC is shown in Fig. 1. Aqueous dispersions of DEPE can undergo a gel to liquid-cryst-

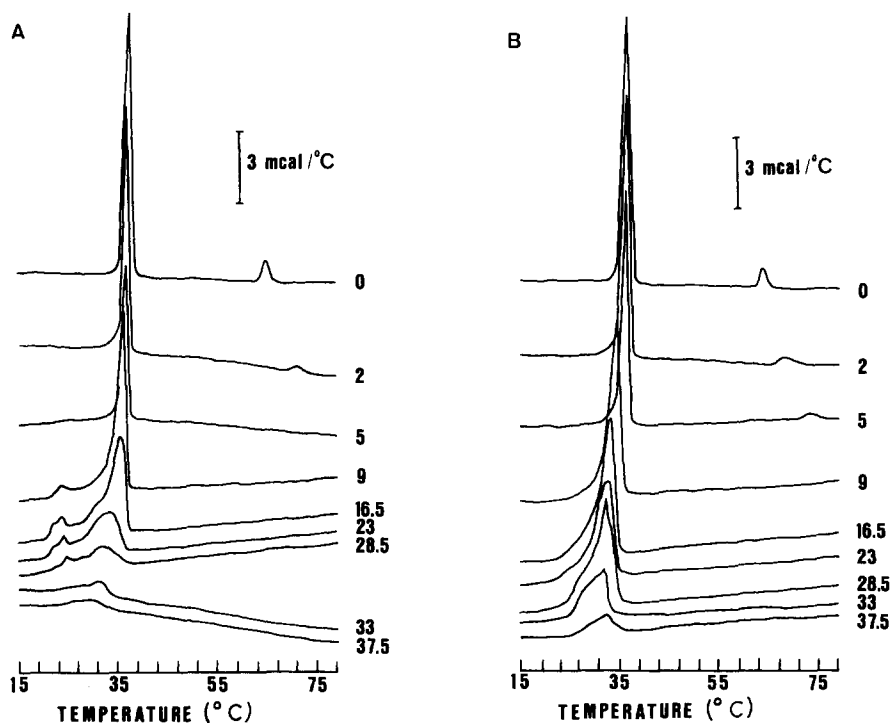


Fig. 1. DSC calorimetric curves for systems containing DEPE and (A) PAF or (B) LPAF. Molar percentages are indicated on the curves. The profiles correspond to heating scans.

talline ( $L_\beta \rightarrow L_\alpha$ ) phase transition in the lamellar phase and in addition a lamellar to hexagonal  $H_{II}$  ( $L_\beta \rightarrow L_H$ ) phase transition [23], as it is shown in the thermograms of pure DEPE (Fig. 1, upper part). The gel to liquid-crystalline phase transition occurred at 36°C whereas the bilayer to hexagonal  $H_{II}$  transition occurred at 63°C in agreement with previous data [23]. The transition enthalpy of the hexagonal  $H_{II}$  transition is much lower than the  $L_\beta \rightarrow L_\alpha$  transition due to the fluid character of both the lamellar and the hexagonal  $H_{II}$  phases [24]. The phase transitions of PAF, LPAF and LPC are known to be much lower than that of DEPE (Refs. 25,26, and our results not shown). Moreover, the transition which occurs in these molecules is from a lamellar (gel) to a micellar (fluid) phase.

The effect of increasing concentrations of PAF in DEPE is shown in Fig. 1A. At lower concentrations of PAF ( $\leq 5$  mol%), the liquid-crystalline chain melting transition profile was not affected significantly, whereas the effect on the bilayer to hexagonal  $H_{II}$  phase transition was more pronounced. These lamellar to hexagonal  $H_{II}$  transitions were shifted to higher temperatures and simultaneously, a decrease in the area and a broadening of the transition were observed. At higher concentrations ( $> 5$  mol%), PAF produced a more complex calorimetric profile (Fig. 1A). Incorporation of increasing amounts of PAF resulted in a shift of the liquid-crystalline phase transition to lower temperatures, concomitantly with a decrease in the area and a broadening of the transition. At concentrations higher than 37.5 mol% this transition was not longer observed due to micellization of the lipids (see Fig. 3).

In Fig. 1A it is observed that a clear change in the pattern of the transition takes place at 9 mol% of PAF, with a shift of the main transition to lower temperatures, accompanied by a broadening of the peak and

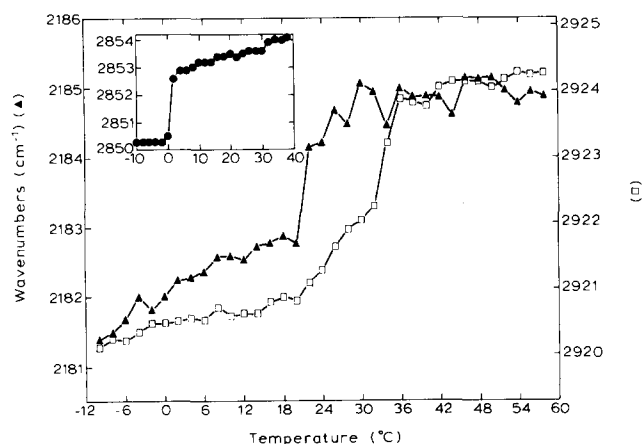


Fig. 2. Temperature dependence of the frequency of the ( $\blacktriangle$ )  $CD_2$  antisymmetric stretching band of dPAF and ( $\square$ )  $CH_2$  antisymmetric stretching band of DEPE/dPAF in a sample containing 16.5 mol% of dPAF in DEPE. The inset shows the transition of pure PAF ( $\bullet$ ).

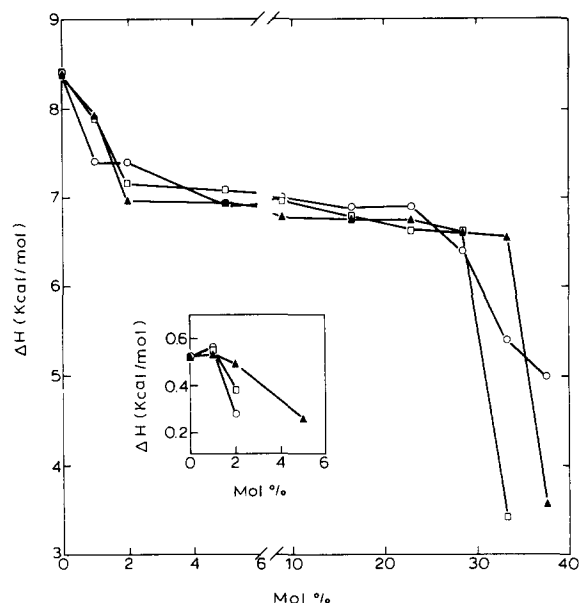


Fig. 3. Dependency of the enthalpy of the main gel to liquid-crystalline phase transition of DEPE upon incorporation of ( $\square$ ) PAF, ( $\blacktriangle$ ) LPAF and ( $\circ$ ) LPC. The inset shows the dependency of the enthalpy of the lamellar to hexagonal  $H_{II}$  phase transition in the presence of ( $\square$ ) PAF, ( $\blacktriangle$ ) LPAF and ( $\circ$ ) LPC.

the appearance of another peak at about 23°C. It has been described that the 1-*O*-octadecyl species of PAF suffers a phase transition at approx. 20°C [26,27] that involves the conformational melting of the alkyl chains. The 1-*O*-hexadecyl PAF species which we are studying here, has a phase transition at 0°C as seen by FTIR (Fig. 2). It is therefore likely that the observed peaks occurring at approx. 23°C correspond to laterally separated phases rich in PAF (see below).

At increasing concentrations of PAF (higher than 9 mol%), the main transition was gradually broadened and a shoulder was observed on the side corresponding to lower temperatures. At 37.5 mol% the transitions were barely discernible and at higher concentrations they were not observed at all.

The effect of the incorporation of LPAF on the phase transitions of DEPE is shown in Fig. 1B. The gel to liquid-crystalline phase transition was affected in a similar way as before in the presence of PAF but significantly, the small endothermic peaks which appeared at 23°C in the presence of PAF were not seen in the presence of LPAF. The effect of the incorporation of LPC on the gel to liquid-crystalline phase transition of DEPE was similar to what was found for LPAF (not shown).

In order to discern whether LPAF or LPC were able of forming laterally separated phases from the bulk of DEPE, other DSC experiments were carried out similar to those described for LPC/dipalmitoylphosphatidylcholine mixtures by Van Echteld et al. [28]. Samples including either 16.5 mol% of LPAF or LPC in

DEPE were supercooled to  $-10^{\circ}\text{C}$  and then scanned by heating up to  $75^{\circ}\text{C}$ . In another experiment samples were first frozen in the calorimeter at  $-15^{\circ}\text{C}$  and then heated to  $2^{\circ}\text{C}$  to melt isothermally the ice. It was subsequently supercooled to  $-10^{\circ}\text{C}$  and then the heating scan was recorded. In none of these cases (not shown), transitions different from those shown in Fig. 1B were found. Therefore, neither LPAF nor LPC appear to be able of forming laterally segregated phases when mixed with DEPE. Similar cooling and heating experiments were also carried out for PAF and again the only transitions detected were those shown in Fig. 1A.

The effect of increasing concentrations of LPAF in the lamellar to hexagonal  $H_{II}$  phase transition of DEPE was different in some aspects to what was found for PAF and LPC. At a concentration of 5 mol% of LPAF, it was still possible to observe an endothermic peak at approx.  $71^{\circ}\text{C}$  which corresponds to the lamellar to hexagonal  $H_{II}$  phase transition of DEPE. This transition was completely absent in DEPE in the presence of 5 mol% of PAF (compare Figs. 1A and 1B) or 5 mol% of LPC (results not shown). Apart from that, 9 mol% of LPAF or LPC induced a shift towards lower temperatures of the transition, and this shift is still higher at 16.5 mol%. Higher concentrations did not further shift the center of the transition peak. Similarly to the effect described for PAF, increasing concentrations of LPAF or LPC, higher than 5 mol%, gradually broadened the transition peak making it barely visible. At 41 mol% the transition was not detectable at all.

It has been shown above that DEPE/PAF, but neither DEPE/LPAF nor DEPE/LPC mixtures, presented two different endothermic peaks in the DSC thermograms (Fig. 1). FTIR has been employed in order to verify the assumption that they corresponded to laterally separated phases, one of them rich in PAF. The phase transition of phospholipids can be conveniently monitored through the shift in frequency of their  $\text{CH}_2$  stretching bands as seen in the FTIR spectrum [29]. In order to overcome the problem of band overlapping, we have used PAF specifically deuterated in the hydrocarbon chain, dPAF. In this way, the phase transition of DEPE and dPAF in the same mixture can be observed through changes in frequency of their  $\text{CH}_2$  and  $\text{CD}_2$  stretching modes, respectively. As seen in Fig. 2 for 16.5 mol% dPAF in DEPE, a transition was observed for the  $\text{CD}_2$  stretching band, which corresponds to dPAF, at approx.  $22^{\circ}\text{C}$ . On the other hand, the  $\text{CH}_2$  stretching band presented two different transitions, one beginning at approx.  $21^{\circ}\text{C}$  and the other one at  $32^{\circ}\text{C}$ , which is in accordance with the DSC data (see Fig. 1). It should be noted that the  $\text{CH}_2$  stretching band arises essentially from DEPE, although a minor contribution corresponds to the  $\text{CH}_2$  stretching mode of dPAF. As DEPE has two acyl chains and dPAF only

one alkyl chain but including several C-D bonds, dPAF accounts for less than 8% of the total signal.

Although the presence of multiple transition peaks in DSC thermograms of a binary lipid mixture is not conclusive evidence of phase separation [30], these FTIR results confirm the existence of laterally separated phases in the presence of PAF: the endotherm appearing at lower temperatures (approx.  $23^{\circ}\text{C}$ ) corresponds to a PAF-rich phase whereas the endotherm appearing at higher temperatures (approx.  $33^{\circ}\text{C}$ ) corresponds to a DEPE-rich phase. Some molecules of PAF should be expected to partition into the DEPE-rich phase melting at  $32^{\circ}\text{C}$  because this transition is taking place at a lower temperature and it is broadened compared to pure DEPE. Therefore a second transition at approx.  $32^{\circ}\text{C}$  should be expected for PAF. This is not clearly observed in Fig. 2 due to the considerable scattering of the data at these temperatures. It should be taken into account to understand this scattering that the bands arising from dPAF were of very low intensity due, first, to its low concentration in the sample and second, to the fact that the signal intensity was originated from only a few C-D bonds in the molecule.

The effects of PAF on  $\Delta H$  of the transitions are shown in Fig. 3.  $\Delta H$  of pure DEPE was found to be 8.3 kcal/mol for the gel to liquid-crystalline phase transition and 0.7 kcal/mol for the bilayer to hexagonal  $H_{II}$  phase transition (see insert of Fig. 3) in agreement with previous data [23]. It is remarkable that  $\Delta H$  of the main transition suffered a steep decrease in samples with PAF concentrations up to 2 mol% (Fig. 3). However, the value of  $\Delta H$  remained nearly constant from 2 to 30 mol% with only a small decrease, despite the broadening of this transition in this concentration range (see Fig. 1A).  $\Delta H$  steeply decreased again at concentrations above 30 mol% of PAF, becoming finally not detectable at concentrations above 33 mol%. The suppression of the phase transition by relatively high concentration of PAF can be explained by the micellization of the lipids. The behavior of  $\Delta H$  for LPAF and LPC samples was similar to what was found for PAF (Fig. 3).

The effect of PAF, LPAF and LPC on the phase behavior of DEPE was investigated by means of  $^{31}\text{P}$ -NMR. Phospholipids give rise to a characteristic asymmetrical  $^{31}\text{P}$ -NMR line-shape with a high-field peak and a low-field shoulder when they are organized in bilayer structures presenting a residual chemical shift anisotropy ( $\Delta\sigma$ ) of approx. 64 ppm in the gel state and approx. 42 ppm in the liquid-crystalline state [31,32]. But, in the hexagonal  $H_{II}$  phase, due to rapid lateral diffusion of the phospholipids around the tubes of which this phase is composed, the chemical shift anisotropy is averaged resulting in a shape with reverse asymmetry when compared to the bilayer line-shape, i.e., a high-field shoulder and a low-field peak with

approximately a 2-fold reduction in the absolute value of  $\Delta\sigma$  [22,33].

The  $^{31}\text{P}$ -NMR of pure DEPE is shown in Fig. 4A. In the lamellar state, pure DEPE presents an asymmetrical  $^{31}\text{P}$ -NMR line-shape with a high-field peak and a low-field shoulder, whereas in the hexagonal  $\text{H}_{\text{II}}$  phase it presents an asymmetrical line-shape with a high-field shoulder and a low-field peak (Fig. 4A). Characteristically,  $\Delta\sigma$  in the gel state is greater than in the liquid-crystalline state due to increased  $^1\text{H}$ - $^{31}\text{P}$  dipolar interactions [34] (compare spectra at 27°C and 37°C).

The presence of 2 mol% of PAF in DEPE results in spectra very similar to those of pure DEPE (not shown). Incorporation of increasing concentrations of PAF induced two different effects on the  $^{31}\text{P}$ -NMR spectra of DEPE. As seen in Fig. 4B, the incorporation of 16.5 mol% of PAF induced, first, the appearance of an isotropic component visible at all temperatures, and second, it abolished the lamellar to hexagonal  $\text{H}_{\text{II}}$  phase transition, at least in the temperature range studied ( $\leq 75^\circ\text{C}$ ), in agreement with the DSC results (see above). The appearance of an isotropic component in the presence of PAF indicates that part of the phospholipid molecules experience a rapid motion that leads to a nearly complete averaging of the chemical shift anisotropy. This effect is more apparent at higher concentrations of PAF as shown in Fig. 4C for 28.6 mol% of PAF in DEPE. In this case the isotropic component is the major one, but a lamellar component is still visible at all temperatures studied. The isotropic component which is observed at this concentration is originated from micelles as demonstrated by observing

the  $^{31}\text{P}$ -NMR spectra of supernatants and pellets of this sample (not shown, see Materials and Methods), whereas the isotropic component which was observed at lower concentrations was not due to the formation of micelles (no  $^{31}\text{P}$ -NMR signal was observed in the supernatants). The formation of micelles coincides with the sharp decrease in enthalpy observed by DSC (Fig. 3).

The effect of the incorporation of LPAF on the  $^{31}\text{P}$ -NMR spectra of DEPE is nearly identical to what has been shown above for PAF (results not shown).

The presence of 2 mol% of LPC in DEPE resulted in spectra very similar to pure DEPE, but significantly, a small isotropic component is present in the hexagonal  $\text{H}_{\text{II}}$  state but not in the lamellar state. This behavior is completely different to that found before for PAF and LPAF (results not shown for this concentration). Incorporation of increasing concentrations of LPC induced two different effects on the  $^{31}\text{P}$ -NMR spectra of DEPE. The incorporation of 16.5 mol% of LPC induced the appearance of a small isotropic component, visible at all temperatures, and abolished the lamellar to hexagonal  $\text{H}_{\text{II}}$  phase transition in the temperature range studied ( $\leq 75^\circ\text{C}$ ). This effect was more apparent at higher concentrations of LPC as shown in Fig. 4D. In contrast to the patterns observed for PAF and LPAF, the lamellar component was still the major one at lower temperatures for 33.3 mol% of LPC in DEPE (Fig. 4D). The isotropic component which was observed at this concentration is originated from micelles, whereas the isotropic component which appeared at lower concentrations was not due to the

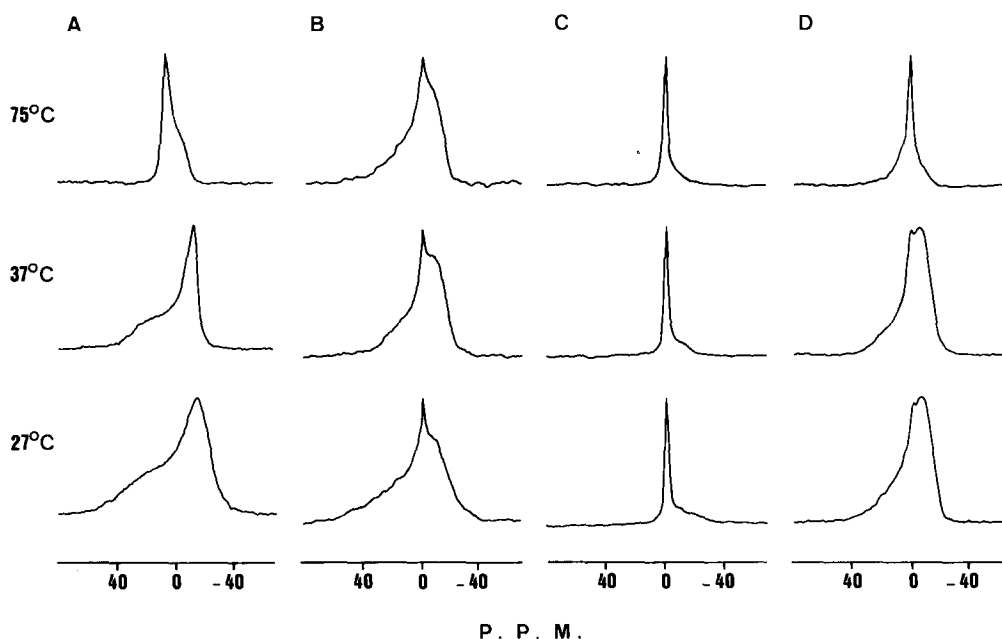


Fig. 4.  $^{31}\text{P}$ -NMR spectra of (A) pure DEPE and DEPE containing (B) 16.5 mol% PAF, (C) 28.58 mol% PAF and (D) 33.3% LPC at the temperatures indicated. The spectra have been normalized to the same signal height.

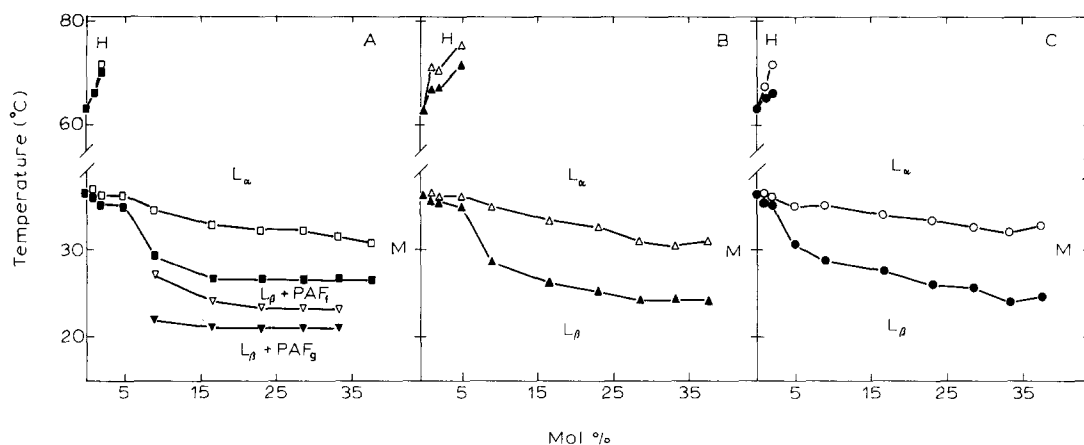


Fig. 5. Partial phase diagrams for systems containing DEPE and (A) PAF, (B) LPAF and (C) LPC. Closed and open symbols were obtained from DSC heating and cooling scans respectively. L, lamellar, H, hexagonal  $H_{II}$  and M, micellar phases.

formation of micelles (no  $^{31}\text{P}$ -NMR signal was detected in supernatants). The formation of micelles in the presence of LPC took place also at the same concentration than the sharp decrease in enthalpy was seen by DSC (Fig. 3).

Partial phase diagrams have been constructed on the basis of DSC and  $^{31}\text{P}$ -NMR results. DSC onset temperatures for the liquid-crystalline transition ( $T_c$ ) and for the bilayer to hexagonal  $H_{II}$  transition ( $T_H$ ) have been used as primary data. Heating and cooling DSC scans were used to produce the solidus and fluidus lines respectively, as described before [35].

The phase diagram corresponding to mixtures of PAF with DEPE is shown in Fig. 5A. It can be seen that a good mixing takes place up to 5 mol%. At higher concentrations, phase separation takes place, with mixtures rich in PAF being laterally separated. At concentrations higher than 37.5 mol% of PAF the system is solubilized. On the other hand,  $T_H$  gradually increases until 2 mol% of PAF. At higher concentrations this transition is not longer observable, at least in the range of temperatures studied here.

Similar patterns were found for LPAF/DEPE and LPC/DEPE mixtures (Figs. 5B and 5C, respectively). In the case of LPAF/DEPE systems phase separation seems to start at concentrations higher than 5 mol% but in the case of LPC/DEPE systems it occurs above 3 mol%. At higher concentrations than 37.5 mol% the systems were solubilized in micelles.

## Discussion

We have studied in this work the interaction of PAF, LPAF and LPC with DEPE. The three molecules, i.e., PAF, LPAF and LPC, share the characteristic of being asymmetrical with a relatively large polar group and a relatively small hydrophobic part (only one hydrocarbon chain compared with the common phosphoglycerides which have two hydrocarbon chains). This type of inverted cone-shaped molecules are expected

to stabilize lamellar phases with respect to hexagonal  $H_{II}$  phases [24]. This effect was in fact observed for LPC/DEPE mixtures [36] and interpreted in this sense. The relative stability of bilayer and non-bilayer phases is determined by some factors, such as the intrinsic radius of curvature of each monolayer of a bilayer and the relief of hydrocarbon packing constraints in the  $H_{II}$  phase [37,38]. Considering the shape of these molecules, they are expected to decrease the intrinsic radius of curvature and to increase the packing constraints in the  $H_{II}$  phase and hence to stabilize the lamellar phase.

It is worthy to note that ether lipids, due to intermolecular attractive forces associated with the ether linkage, would promote the lamellar to hexagonal phase transition [39]. Although PAF and LPAF have ether linkages in their structures, it seems that the effect of their asymmetric shape will be predominant so that they will favor lamellar phases as we have observed here by  $^{31}\text{P}$ -NMR.

It has been described after DSC and spectroscopic measurements that pure PAF and pure LPC exhibit a gel (bilayer) to fluid (micellar) transitions [25–27]. However, when incorporated into DEPE bilayers the thermodynamic behavior of the system is dominated by DEPE, up to about 30 mol% of PAF and 33 mol% of LPAF and LPC, as it can be observed through the DSC patterns (Fig. 1) and the decrease in  $\Delta H$  (Fig. 3) of the gel to fluid (lamellar) transitions. Therefore, at concentrations lower than those, the acyl chains of PAF, LPAF and LPC interact with those of DEPE. Nevertheless, PAF, but neither LPAF nor LPC, is able of producing a lateral phase segregation of phases rich in PAF at concentrations between 9 and 33 mol% (Fig. 1A), this upper concentration limiting the transition between lamellar (fluid) and micellar phases.

$^{31}\text{P}$ -NMR measurements showed that 16.5 mol% of PAF and LPAF were able of inducing the appearance of isotropic signals at all temperatures. These isotropic

signals, originated from lipids forming part of the vesicles, could arise from lipids with unique reorientational motions of the phosphate headgroup, or alternatively, from the formation of nonlamellar structures within the membrane [40].

As presented in the phase diagrams (Fig. 5) the main features of the interaction of PAF with DEPE are as follows. At concentrations higher than 5 mol% phase separations take place, so that PAF rich phases are formed. However, not all PAF molecules are separated from DEPE, since the  $L_\beta$  to  $L_\alpha$  phase transitions are considerably broadened indicating non-ideal lipid mixing. It seems then, that a major reorganization of the membrane takes place at concentrations greater than 5 mol% and lower than 30 mol%. The  $H_{II}$  phase is not detectable (at least in the range of temperatures studied here), some PAF molecules are laterally segregated and the rest of the molecules of PAF which remain mixed with DEPE considerably alter its lamellar structure. It has been described that PAF may form interdigitated structures when mixed with phosphatidylcholines [41]. It is possible that the PAF molecules segregated from the bulk lipids may form such a type of structures when mixed with DEPE giving place to the small transition peaks observed by DSC.

On the other hand PAF, LPAF and LPC show a fluidizing effect on DEPE membranes, as seen by the decrease in the  $L_\beta \rightarrow L_\alpha$  phase transition monitored by DSC, and this is in agreement with what has been seen previously for LPC [13], and PAF and LPAF [42].

In conclusion, the asymmetric lipids PAF, LPAF and LPC, at concentrations at which they do not solubilize the membrane, show a limited miscibility with DEPE membranes. These membranes are quite disrupted at concentrations higher than 5 mol% of PAF or LPAF and 3 mol% of LPC, and, at concentrations higher than those indicated, they are not able of giving  $L_\alpha \rightarrow H_{II}$  phase transitions. Moreover, immiscibilities appear in the membranes: PAF is even able of giving clearly detectable separated phases rich in PAF.

It is finally convenient to make some comments on the interaction of PAF and LPC with lipids since this may be relevant to their biological or pharmacological activities. With respect to PAF, it is known that physiological concentrations are in the nM range which is a extremely low concentration in the membrane. Apart from that, it is known that PAF binds with high affinity to receptors in plasma membranes [1]. However, as PAF is an amphipathic molecule, it may also bind to membranes in a non-specific way. In some in vitro experiments where PAF has been used at pharmacological concentrations, i.e., in the  $\mu M$  range, the PAF/lipid ratios may be as high as 1 at a PAF concentration of 4  $\mu M$  [43]. This means that if PAF is used at these concentrations it may induce a number of alter-

ations in the membrane fluidity [42] and structure (Ref. 41 and this work). Apart from that, it has been described that PAF may be accumulated in some biomembranes, such as phagolysosomal membranes prepared from neutrophils stimulated with opsonized zymosan at concentrations greater than 0.5 mol% [7]. As observed by us, at this low concentration PAF alters the behavior of DEPE stabilizing the lamellar phase.

On the other hand, LPC is a normal component of biological membranes where it may reach concentrations near 2 mol% of total membrane lipid in liver plasma membrane [44]. Again we observe at these concentrations that LPC may stabilize lamellar structures in DEPE, giving a clear alteration in the system. When LPC is used in in vitro experiments in the  $\mu M$  range, it may reach membrane concentrations similar to those mentioned above for PAF, producing then a considerable perturbation of the system, as shown for DEPE membranes in this work.

Apart from that, it can be speculated that both PAF and LPC might reach considerable high local concentrations if they have preference for partitioning in particular membrane domains. Thus, their effective concentrations might be higher than it has been considered so far, leading to membrane perturbations as described in this work.

## Acknowledgements

This work has been supported in part by grant No. PM90-0044 from DGICYT, Spain. J.S. is a recipient of a scholarship from the Basque Government, Vitoria, Spain.

## References

- 1 Prescott, S.M., Zimmerman, G.A. and McIntyre, T.M. (1990) *J. Biol. Chem.* 265, 17381–17384.
- 2 Henson, P.M. (1970) *J. Exp. Med.* 131, 287–304.
- 3 Demopoulos, C.A., Pinckard, R.N. and Hanahan, D.J. (1979) *J. Biol. Chem.* 254, 9355–9358.
- 4 Goetzl, E.J., Derian, C.K., Tauber, A.I. and Valone, F.H. (1980) *Biochem. Biophys. Res. Commun.* 94, 881–888.
- 5 Braquet, P., Touqui, L., Shen, T.Y. and Vargaftig, B.B. (1987) *Pharmacol. Rev.* 39, 97–145.
- 6 Kornecki, E. and Ehrlich, Y.H. (1988) *Science* 240, 1792–1794.
- 7 Riches, D.W.H., Young, S.K., Secombe, J.F., Lynch, J.M. and Henson, P.M. (1985) *Fed. Proc.* 44, 737–740.
- 8 Henson, P.M. (1987) in *New Horizons in Platelet Activating Factor Research* (Winslow, C.M. and Lee, M.L., eds), pp. 3–10, Wiley, Chichester.
- 9 Huang, C. and Mason, J.T. (1986) *Biochim. Biophys. Acta* 864, 423–470.
- 10 Lee, T.C. and Fitzgerald, V. (1980) *Biochim. Biophys. Acta* 598, 189–192.
- 11 Paltauf, F. (1983) in *Ether-lipids: Biochemical and Biomedical Aspects*, (Mangold, H.K. and Paltauf, F., eds.), pp. 309–355, Academic Press, New York.
- 12 Killian, J.A., Borle, F., De Kruijff, B. and Seelig, J. (1986) *Biochim. Biophys. Acta* 854, 133–142.

- 13 Van Echteld, C.J.A., De Kruijff, B., Mandersloot, J.G. and De Gier, J. (1981) *Biochim. Biophys. Acta* 649, 211–220.
- 14 Teruel, J.A., Soler, F. and Gómez-Fernández, J.C. (1991) *Chem. Phys. Lipids* 59, 1–7.
- 15 Saito, T., Wolf, A., Menon, N.K., Sand, M. and Bing, R.J. (1988) *Proc. Natl. Acad. Sci. USA* 85, 8246–8250.
- 16 Quinn, M.K., Parthasarathy, S. and Steinberg, D. (1988) *Proc. Natl. Acad. Sci. USA* 85, 2805–2809.
- 17 Gordon-Kamm, W.J. and Stepoukos, P.L. (1984) *Proc. Natl. Acad. Sci. USA* 81, 6373–6377.
- 18 Navarro, J., Toivio-Kinnucan, M. and Racker, E. (1984) *Biochemistry* 23, 130–135.
- 19 Verkleij, A.J. (1984) *Biochim. Biophys. Acta* 779, 43–63.
- 20 Elias, A.W., Chapman, D. and Ewing, D.F. (1976) *Biochim. Biophys. Acta* 448, 220–230.
- 21 Bartlett, G.R. (1959) *J. Biol. Chem.* 234, 466–471.
- 22 Seelig, J. (1978) *Biochim. Biophys. Acta* 515, 105–140.
- 23 Gallay, J. and De Kruijff, B. (1984) *Eur. J. Biochem.* 142, 105–112.
- 24 Cullis, P.J. and De Kruijff, B. (1979) *Biochim. Biophys. Acta* 559, 399–420.
- 25 Klopfeitein, W.E., De Kruijff, B., Verkleij, A.J., Demel, R.A. and Van Deenen, L.L.M. (1974) *Chem. Phys. Lipids* 13, 215–222.
- 26 Mushayakarara, E.C. and Mantsch, H.H. (1985) *Can. J. Biochem. Cell Biol.* 63, 1071–1076.
- 27 Huang, C., Mason, J.T., Stephenson, F.A. and Levin, I.W. (1986) *Biophys. J.* 49, 587–595.
- 28 Van Echteld, C.J.A., De Kruijff, B. and De Gier, J. (1980) *Biochim. Biophys. Acta* 595, 71–81.
- 29 Casal, H.L. and Mantsch, H.H. (1984) *Biochim. Biophys. Acta* 779, 381–401.
- 30 Mabrey, S. and Sturtevant, J.M. (1976) *Proc. Natl. Acad. Sci. USA* 73, 3862–3866.
- 31 Van Echteld, C.J.A., Van Stigt, R., De Kruijff, B., Leunissen-Bijvelt, J., Verkleij, A.J. and De Gier, J. (1981) *Biochim. Biophys. Acta* 648, 287–291.
- 32 Killian, J.A. and De Kruijff, B. (1985) *Biochemistry* 24, 7881–7890.
- 33 Cullis, P.J. and De Kruijff, B. (1978) *Biochim. Biophys. Acta* 507, 207–218.
- 34 Seelig, J. and Gally, H.V. (1976) *Biochemistry* 15, 5199–5204.
- 35 Phillips, M.C., Ladbrooke, B.D. and Chapman, D. (1970) *Biochim. Biophys. Acta* 196, 35–44.
- 36 Epand, R.M. (1985) *Biochemistry* 24, 7092–7095.
- 37 Gruner, S. (1985) *Proc. Natl. Acad. Sci. USA* 82, 3665–3669.
- 38 Siegel, D.P., Bansbach, J. and Yeagle, P.L. (1989) *Biochemistry* 28, 5010–5019.
- 39 Boggs, J.M., Stamp, D., Hughes, D.W. and Deber, C.M. (1981) *Biochemistry* 20, 5728–5735.
- 40 Cullis, P.R., Hope, M.J. and Tilcock, C.P.S. (1986) *Chem. Phys. Lipids* 40, 127–144.
- 41 Olivier, J.L., Chachaty, C., Quinn, P.J. and Wolf, C. (1991) *J. Lipid Mediators* 3, 311–332.
- 42 Bratton, D.L., Adron, R., Clay, K.L. and Henson, P.M. (1988) *Biochim. Biophys. Acta* 941, 76–82.
- 43 Sawyer, D.B. and Andersen, O.S. (1989) *Biochim. Biophys. Acta* 987, 129–132.
- 44 Shier, W.T., Baldwin, J.H., Nilsen-Hamilton, M., Hamilton, R.T. and Thanassy, N.M. (1976) *Proc. Nat. Acad. Sci. USA* 73, 1586–1590.